Earth and Planetary Science Letters 530 (2020) 115946

Contents lists available at ScienceDirect

Earth and Planetary Science Letters

www.elsevier.com/locate/epsl

Magnetic detection of paleoflood layers in stalagmites and implications for historical land use changes

J.M. Feinberg [a,*], I. Lascu [b], E.A. Lima [c], B.P. Weiss [c], J.A. Dorale [d], E.C. Alexander Jr. [a], R.L. Edwards [a]

[a] Institute for Rock Magnetism, Department of Earth and Environmental Sciences, University of Minnesota, Minneapolis, MN 55455, USA
[b] Department of Mineral Sciences, National Museum of Natural History, Smithsonian Institution, Washington, DC 20560, USA
[c] Department of Earth, Atmospheric, and Planetary Sciences, Massachusetts Institute of Technology, Cambridge, MA 02139, USA
[d] Department of Earth and Environmental Sciences, University of Iowa, Iowa City, IA 52242, USA

ARTICLE INFO

Article history:
Received 16 March 2019
Received in revised form 31 October 2019
Accepted 3 November 2019
Available online 13 November 2019
Editor: L. Robinson

Keywords:
flood recurrence
speleothem
mineral magnetism
scanning SQUID microscopy

ABSTRACT

Flooding events are major natural hazards that present significant risk to communities worldwide. Calculations of flood recurrence rate through time are important tools for regulating land use, determining insurance rates, and for the design and construction of levees and dams. Typically, flood recurrence rates are based on limited historical data or on evidence preserved in the geologic record as overbank deposits, tree ring scars, or high water scour marks. However, these approaches are either limited in their ability to produce continuous time series of flooding events or do not consider the effects of regional land use change. Here we use scanning superconducting quantum interference device (SQUID) microscopy to rapidly image the magnetization associated with flood layers in a polished surface of an annually laminated stalagmite from Spring Valley Caverns (SVC) in southeastern Minnesota. A time series of magnetization peaks, each of which corresponds to a flooding event, yields an average flood recurrence rate of $\leq$5 events per century for the last 500 years. This rate increases to $\sim$7 events per century since 1900, coincident with historical timber and agricultural land-use changes in Minnesota. This approach produces a continuous record of well-dated, extreme-precipitation events that can be examined within the context of land use change.

1. Introduction

Estimates of the frequency of major floods are essential tools for natural hazard planning. They are employed by city planners to zone industrial, agricultural, and residential land uses, by insurance companies for determining coverage rates, and by governmental agencies during the construction of levees and dams (Committee on Levees and the National Flood Insurance Program Improving Policies and Practices, 2013). Modern flood recurrence rates are typically determined using historic records of annual stream flow measurements that extend across the last 150 years. Yet historically-derived flood recurrence rate estimates are prone to uncertainties due to their relatively short duration (often <100 years) and to recent dramatic changes in runoff patterns associated with urban and agricultural drainage systems that more efficiently channel rain and melt water toward rivers. Efforts to understand how flood recurrence has changed over timescales longer than 150 years often rely upon paleoflood indicators such as tree scars and tree ring features (St. George and Nielsen, 2002, 2003), overbank and slack-water deposits (Knox, 1985, 1993, 2000), and high-water scour marks (Baker, 1973), all of which are difficult to compile into continuous histories of flooding.

Here we demonstrate that rock magnetic techniques can be used to rapidly identify major flooding events preserved within stalagmites and that these well-dated cave records can in turn be used to compile accurate regional flood recurrence rates extending back in time thousands of years. Flood records preserved within speleothems offer a number of advantages over existing paleoflood indicators. The continuous growth of speleothems provides a time series of hydrologic behavior. Hiatuses in calcite growth can be recognized and avoided by careful inspection of samples. Speleothems <650 ka in age can be reliably dated radioisotopically with very high precision using ^{230}Th dating techniques (Edwards et al., 2003; Dorale et al., 2004; Cheng et al., 2013). Additionally, the precise year of flooding events in actively growing speleothems that display annual growth laminations can be independently es-

* Corresponding author.
E-mail address: feinberg@umn.edu (J.M. Feinberg).

https://doi.org/10.1016/j.epsl.2019.115946
0012-821X/

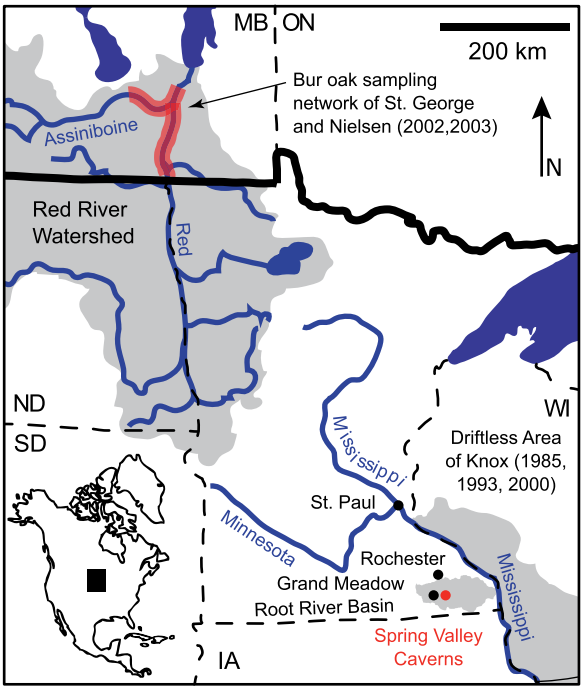

Fig. 1. Map of cave location and watersheds relevant to this study. Red dot shows the location of Spring Valley Cavern, while grey areas show the extent of the Root and Red River watersheds as well as the "Driftless Area" studied by Knox (1985, 1993, and 2000). Black dashed (solid) lines indicate state/province (international) boundaries. Inset in lower right shows region of study within North America. (For interpretation of the colors in the figure(s), the reader is referred to the web version of this article.)

tablished by counting the laminations using confocal fluorescence microscopy (Dasgupta et al., 2010).

We focus on speleothems from Spring Valley Caverns in Minnesota (Fig. 1), where flood layers were recently identified in stalagmites that grew over the last 3000 years (Dasgupta et al., 2010). Such layers form when mineral- and organic-rich detritus adheres to the surface of a stalagmite when it is inundated by flood waters. A flood layer is preserved by the subsequent deposition of calcite once water levels have receded and again exposed the stalagmite. This detritus typically consists of allochthonous silicate grains, with minor concentrations of oxides such as ilmenite and titanomagnetite (Strauss et al., 2013), where thicker flood layers (>200 μm) can be observed on polished surfaces as dark bands that delineate growth horizons (Fig. 2a).

Paleoflood reconstructions from speleothems are a relatively new and underutilized tool (Denniston and Luetscher, 2017) and until now have relied on identifying detrital elements/minerals using laser ablation ICP-MS (Dasgupta et al., 2010; González-Lemos et al., 2015), X-ray diffraction (Gazquez et al., 2014), X-ray fluorescence (Finné et al., 2014), or fluorescence microscopy (Frappier et al., 2014). This earlier work also demonstrated that speleothem samples collected from the same passageways produce similar paleoflood chronologies. However, collecting profiles provides only a one-dimensional view of flood layers within a speleothem, and is time-consuming. Here we report an alternative approach that rapidly maps the two-dimensional distribution of paleoflood events in speleothems by making use of magnetic minerals preserved within flood layers. We use scanning superconducting quantum interference device (SQUID) microscopy in order to achieve the spatial resolution necessary to resolve individual flood events. This case study demonstrates how magnetic measurements on speleothems can be used to infer paleoenvironmental information (Lascu and Feinberg, 2011).

2. Study site, materials, and methods

Spring Valley Caverns (SVC) is situated in Fillmore County in southeastern Minnesota (43°44′24″N, 92°24′36″W) about 6.4 km northwest of the town of Spring Valley (Fig. 1). The cave is located in the Root River watershed of the Upper Mississippi Valley, (Fig. 1). Prior to the onset of widespread European-American settlement in the 1850s, the native vegetation of the area was oak savanna, but is now largely under row crop agriculture. The stalagmite examined in this study (SVC982) is the same carefully dated specimen as used by Dasgupta et al. (2010) and its magnetic mineralogy was described by Strauss et al. (2013). It was originally collected from the wall of a 915-meter long side passage, approximately 1 m in width and 2 m in height, located at a depth of 21 m below the land surface. The passageway leads to a dead-end and is not a major through-going conduit. During flood events, waters would back up into the passageway submerging the stalagmite and then eventually drain away afterwards. This stalagmite was growing with active drips from the ceiling during the time of its collection, and while its vertical orientation is well constrained, it is azimuthally unoriented. A 100 μm-thick section was prepared for scanning SQUID microscopy using non-magnetic polishing equipment (Fig. 2a).

Scanning SQUID microscopy is a tool for high resolution mapping of remanent magnetization in samples (Weiss et al., 2007; Lima and Weiss, 2016). The SQUID microscope uses a monolithic directly coupled niobium based planar SQUID with a field sensitivity of ∼0.01 nT at a frequency of ∼0.01 Hz (Baudenbacher et al., 2003; Fong et al., 2005; Weiss et al., 2007). It measures the vertical component of the magnetic field produced above polished surfaces. Measurements with the SQUID microscope were taken inside a magnetic shield (DC field <40 nT) in the MIT Paleomagnetism Laboratory as planar grids with 100 μm spacing at a sensor-to-sample distance (and approximate horizontal spatial resolution) of 200 μm. Measurements were collected of a 1 T isothermal remanent magnetization (IRM) imparted normal to the polished surface.

3. Results

Measurements of the stray field resulting from the 1 T IRM clearly delineate the presence of individual flood layers (Fig. 2b). Each layer extends from the nearly horizontal splash surface to the sides of the speleothem, tracing its paleo-surface at the time of the flooding event. The intensity of each flood layer's magnetization decreases towards the center of the splash surface, resulting from the partial erosion of allochthonous flood material from the splash surface after drip water conditions were reestablished.

The field data shown in Fig. 2b were inverted using a Fourier algorithm (Lima et al., 2013) to determine the distribution of magnetization within the speleothem (Fig. 2c). This inverted dataset provides finer spatial information about the flood layers within the speleothem. By integrating the magnetization along a profile in Fig. 2c, we calculate the average IRM intensity for calcite layers that grew at a particular moment in time. Stacking consecutive average IRM intensities allows us to produce a time series of IRM peaks, where a peak corresponds to an individual flooding event or a series of closely spaced events (Fig. 3). The SVC982 speleothem produces a record of 22 flooding events (1547, 1592, 1656, 1670, 1693, 1707, 1714, 1723, 1745, 1762, 1766, 1787, 1793, 1850, 1856, 1909, 1919, 1928, 1944, 1959, 1982, 1987), with an average recurrence rate of ≤5 per century for the last 500 years, with 7 events occurring in the 20th century. While the layer counting history for this speleothem is highly accurate (Dasgupta et al., 2010), we estimate an error of ±2.5 years for each flood event associated with minor positioning errors.

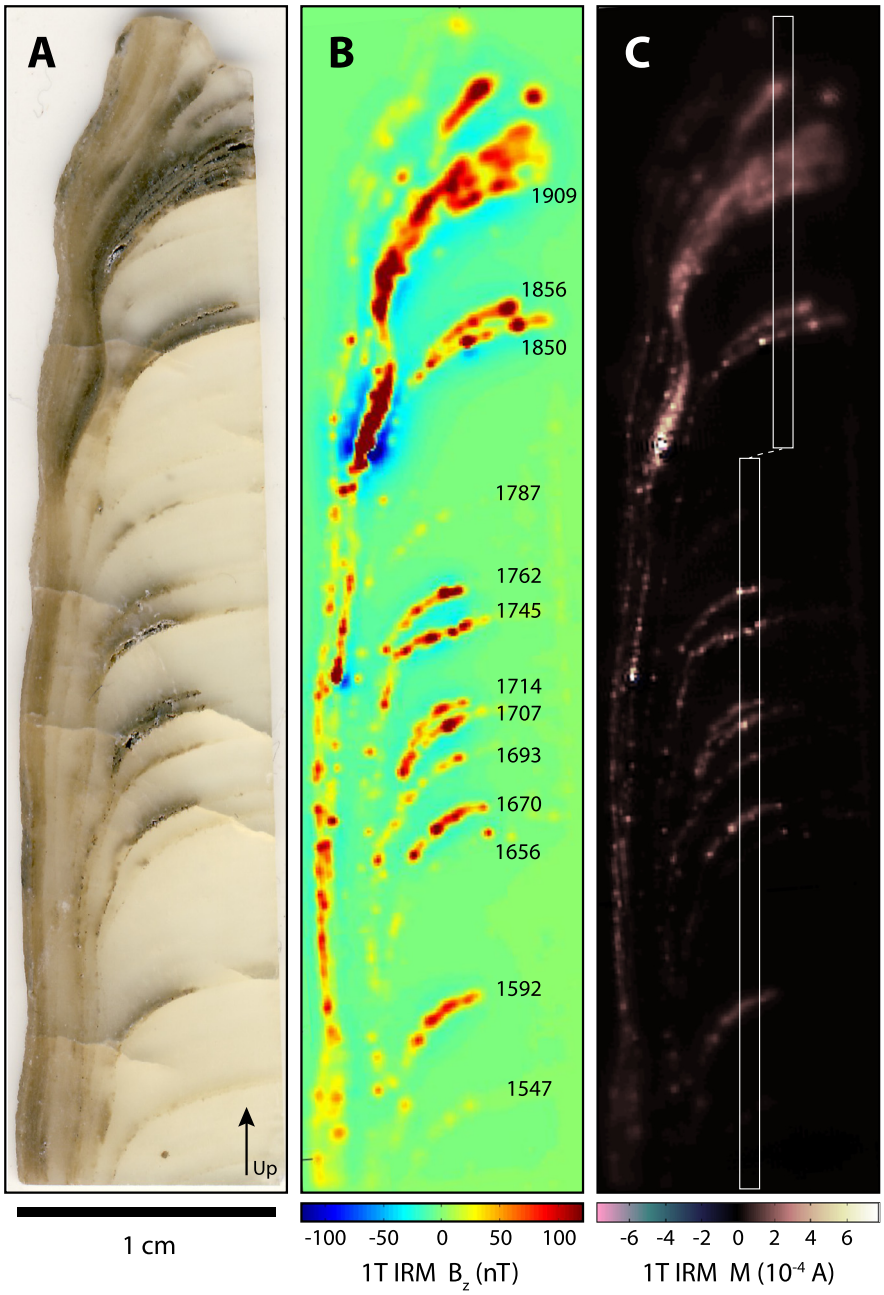

Fig. 2. SQUID microscopy data of the SVC982 stalagmite from Spring Valley Caverns, Minnesota. (a) Plane polarized light image of a radial slice of SVC982, (b) IRM field map with ages of major flood layers, (c) Planar (vertically-integrated) magnetization (moment per unit area) as inferred from inversion of data in (b), with the integrated area for profile in Fig. 3 shown in white boxes. Data in (b) are vertical component of the magnetic field measured at a sensor-to-sample distance of ∼200 μm. Data in (b) and (c) were collected on a 100-μm thin section produced from an immediately adjacent slice to that shown in (a).

4. Discussion

4.1. Comparison with regional flood records

The SVC paleoflood record is consistent with earlier studies on the paleoflood history of the Upper Midwest (e.g., Knox, 1985, 1993, 2000; St. George and Nielsen, 2002, 2003; Dasgupta et al., 2010; Fig. 3a). Knox (1985, 1993, 2000) used overbank flood deposits to show that over the last 7000 years, the mean magnitude and frequency of floods in southwestern Wisconsin varied considerably and noted that recurrence rate estimates over long intervals could not be calculated under the assumption of a fixed mean. Knox (1985) also found that modern floods were larger in magnitude than those that occurred under natural land cover earlier in history. St. George and Nielsen (2002, 2003) used tree ring features to chronicle variable flood rates and intensities within the Red River watershed in Minnesota and Manitoba and observed an increase in flooding events between 1950 and 2000. There are large differences in the size of the catchments that produce these two datasets (Red River watershed: 287,499 km^2, Root River watershed: 4302 km^2, catchment feeding Spring Valley Caverns: 2 km^2) and the study area of St. George and Nielsen (2002, 2003) is located 800 km to the north in a different ecological setting than the Root River watershed.

Additionally, the nature of the flooding events in the two records is slightly different. The flooding events in Spring Valley Caverns are likely to be due to short-lived extreme hydrologic

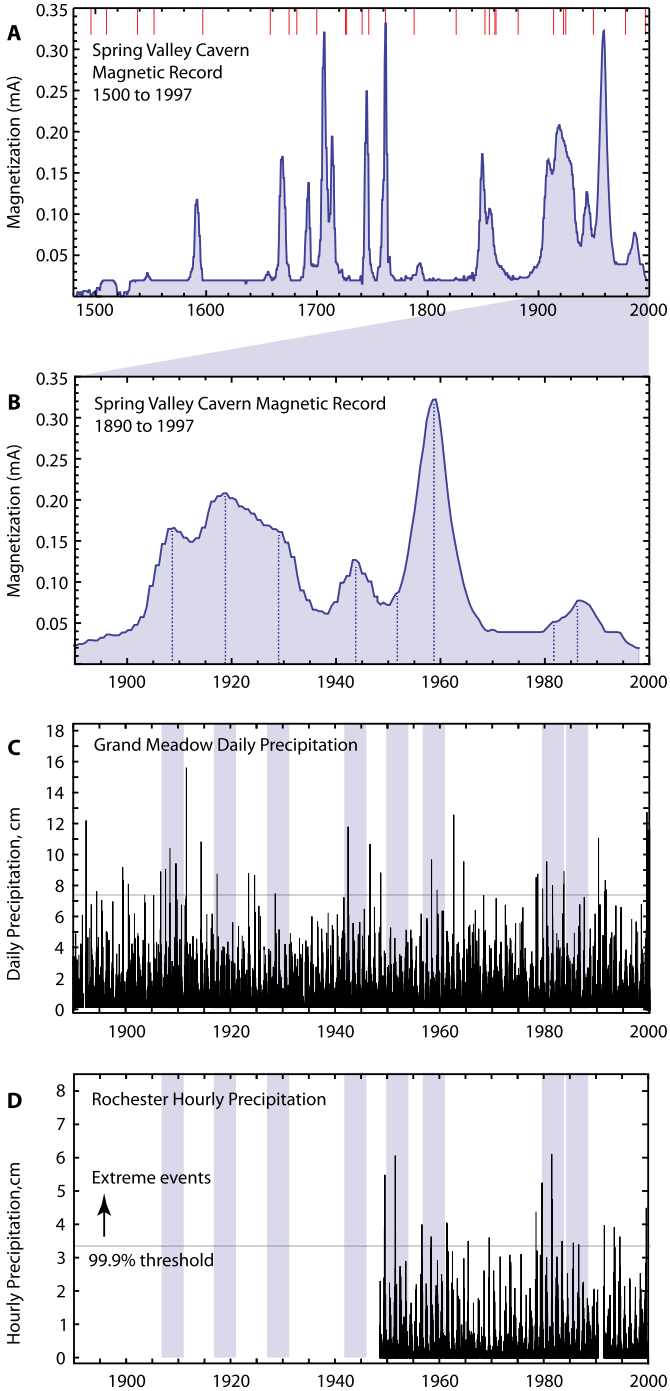

Fig. 3. Paleoflood history at Spring Valley Caverns and comparison to regional precipitation records. (a) Time series of the last four centuries of magnetization along the integrated area from the boxes in Fig. 2c. Peaks show the presence of flood layers preserved within the speleothem. Red lines show the flood layers observed in the Red River Valley Watershed by St. George and Nielsen (2002, 2003) (b) Close-up of 1890-1997. (c) Daily precipitation record from Grand Meadow, Minnesota located 13 km from SVC. The horizontal grey line at 7.6 cm (3.0 inches) indicates the threshold daily precipitation value that encompasses 99.9% of all non-zero precipitation values. Values above this line are considered 'extreme' precipitation events. The vertical bands indicate the position of magnetization peaks ±2.5 years. (d) Hourly precipitation record from Rochester International Airport (18 km form SVC) from 1948-present. The horizontal grey line is the 99.9% threshold value (3.3 cm, 1.3 inches) that defines extreme hourly precipitation events.

events, such as strong thunderstorms or rapid snow melts, where water is unable to drain rapidly enough through the karst conduits and instead backs up behind narrow constrictions in the cave system. By contrast, the flood records compiled by St. George and Nielsen (2003) are based on anatomical features in burr oak (reduced earlywood vessels) that occur when a tree experiences prolonged inundation during spring and early summer.

Therefore, even though both catchments are located in the Upper Midwest of North America, there is no reason to expect that all the floods in the Red River system should also appear in the Spring Valley Caverns record. However, a Kolmogorov-Smirnov test comparing the tree ring paleoflood records from St. George and Nielsen (2002, 2003) to the magnetic record at Spring Valley Cavern record yields a 98.4% probability that the flooding histories are drawn from the same distribution. To further test this relationship, we compared the tree ring flood history to randomly-drawn, uniformly-distributed datasets that were identical in length to the magnetic record at Spring Valley Caverns. This Monte Carlo approach was repeated 10,000 times and produced lower probabilities in 97.2% of the trials. Thus, the level of coherence between the two paleoflood records appears to be statistically significant, and indicates that despite their differences in area and geography, the Red and Root River basins experienced broadly similar paleoflood histories that can be interpreted across a regional spatial scale.

4.2. Comparison to historical precipitation records

To test whether extreme precipitation events influenced the occurrence of flood layers preserved in SVC982, we examined historical daily and hourly precipitation records from two nearby stations. Over the period 1890 to 2000, six out of eight flooding events in the SVC speleothem occur at times of unusually high daily precipitation as measured in nearby Grand Meadow (NCDC station USC00213290) located 13 km due west of SVC (Figs. 1 and 3). For this study, an 'extreme' daily precipitation event was defined as any day with precipitation higher than 99.9 % of all rainy days (7.6 cm or 3.0 inches per day). An hourly precipitation record has been maintained at Rochester airport located 18 km north of SVC from 1948 to the present (WBAN station 14925). Each of the four flood layers identified in the SVC speleothem record during this interval overlaps (within their ±2.5 year error) with extreme hourly precipitation events, including the two flooding events that did not correlate with high daily precipitation events in the Grand Meadow record. Extreme hourly precipitation is defined as being greater than 99.9% of all rainy hourly rates (3.3 cm or 1.3 inches per hour) (Fig. 3). Thus, every flooding event preserved in SVC982 that is younger than 1890 appears to correlate with an extreme daily or hourly rainfall event.

4.3. Climate and land use

Earlier studies have attempted to deconvolve the relative contributions of climate change and land use to varying sedimentation patterns in lakes and rivers in the upper Midwest over the last 1,000 years (e.g., Dasgupta et al., 2010; Umbanhowar et al., 2011). This is a nontrivial task that ultimately will require integration of multiple proxies for natural and anthropogenic processes. At a qualitative level, while it is clear that there has been at least moderate climate change over this period, there is a comparatively dramatic land use change. The magnetic record of SVC982 provides a unique opportunity to assess the relative contributions of both climate and land use to the flooding record in Spring Valley Caverns.

Prior to the late 1800s, the magnetization peaks associated with flooding events appear as narrow, discrete, well-constrained peaks. After the late 1800s, the magnetization peaks change and appear broader (Fig. 4) despite being of the same magnitude, and tend to overlap one another, making it more difficult to constrain the

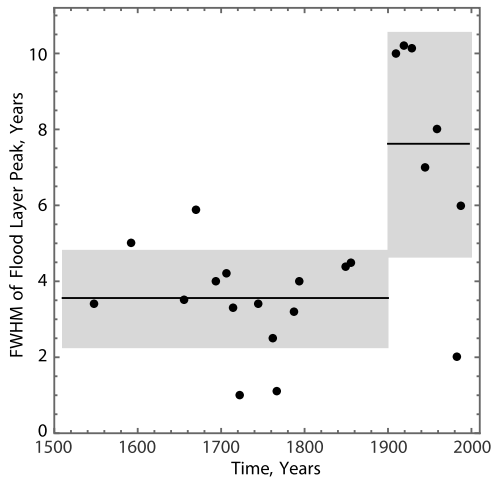

Fig. 4. Width of paleoflood magnetization peaks vs. time. The full-width half maximum (FWHM) values change from an average of ∼3.5 years before 1900 to ∼7.5 years after 1900. The gray zones indicate the one standard deviation error on the mean peak width.

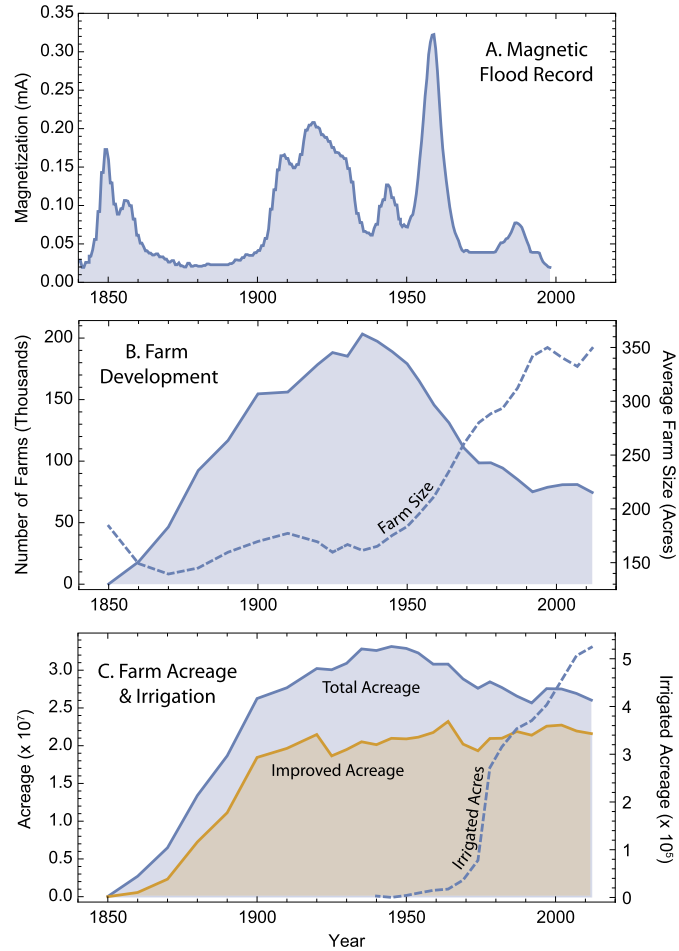

Fig. 5. Land use history in Minnesota. (a) The magnetization record from 1840 to 1998 in the Spring Valley Caverns stalagmite. (b) The evolution of the number of farms in Minnesota and their average size. (c) the progressive increase in total farm acreage and actively farmed ("improved") acreage, which reaches a plateau ∼1900. Groundwater irrigation began quietly during the 1940s, but accelerated dramatically during the 1970s and early 2000s (note the factor of 100 between the left and right vertical scales.

precise age of any single flooding event. Here, we argue that this transition after the late 1800s is a reflection of broader historical land use trends active across much of Minnesota associated with the influx of European-American settlers into the upper Midwest.

Fig. 5 shows a history of farming practices in the state of Minnesota, as documented by state census data from 1850 to 2012. The influx of settlers into the territory of Minnesota began in the early 1820s. To meet their needs for heating and building materials, as well as those of other communities as far south as Saint Louis, settlers immediately began to deforest the area by timber cutting (Larson, 2007). Deforested areas were converted to farmland and, shortly thereafter, the number of farms began to accelerate from only 157 in 1850 to 18,181 in 1860. The peak number of farms occurred in 1935 with just over 200,000. During this same interval, the total farming acreage in the state reached its peak and the area of "improved acreage" (all land that is regularly tilled or mowed, pasture, fallow, gardens, orchards, vineyards, and areas containing farm buildings) has remained roughly steady since 1910 (Fig. 5c). During the 1930s and 1940s, the development of mechanized farming allowed fewer people to efficiently manage larger areas, and consequently the number of Minnesota farms began to decrease, while the average farm size increased (Fig. 5b). In addition, mechanized framing enabled ploughing to greater soil depths. The use of groundwater irrigation systems began as a slow trickle in the 1940s, but expanded most dramatically during the 1970s and early 2000s (Fig. 5c).

Some of these changes in land use had a profound effect on the rate in which precipitation and snowmelt was channeled to first order streams and led to increased suspended sediment loads in Minnesota rivers (Novotny and Stefan, 2007; Engstrom et al., 2009). In karstic regions, these land use changes are also likely to increase the rate at which water is introduced into the subsurface through overland flow to sinking streams and sinkholes. Additionally, diffuse infiltration though the soil and into the underlying epikarst (autogenic and allogenic recharge) is also likely to increase. Ploughing effectively breaks up soil peds and hard pans, and homogenizes previously formed soil horizons, making it easier for minute soil particles to be translocated into the subsurface or suspended in overland flow during storm events. Ploughing also effectively increases the infiltration rate of soil allowing precipitation to diffuse into the epikarst more rapidly and deliver higher concentrations of sediment to the subsurface. Initial land use changes in Minnesota associated with the timber industry and nascent agriculture in the 1850s may have contributed to the magnetization peaks centered at 1850 and 1856. The dramatic expansion of farms leading up to 1910 and subsequent changing agricultural practices (e.g., change from horse-drawn plows to mechanized farming) are correlated in time with increased magnetic material in the speleothems at SVC, including broader magnetization peaks and higher baseline magnetic background values. While the record at SVC only captures land use changes associated with the farmland immediately overlying the cavern, it serves as a microcosm of larger societal land use changes that were active throughout Minnesota's recent history.

Settlements in the Red River Valley experienced a similar land use history to southeastern Minnesota, offering an explanation for why both regions record similar flooding histories. Significant areas were deforested by a rapidly growing timber industry in the 1850s (Ross, 1856), and row crop farming spread widely throughout the early half of the 20th century.

5. Conclusions

Our rock magnetic investigation of the SVC982 stalagmite at Spring Valley Caverns has yielded an exceptionally well-dated record of extreme precipitation events in southeastern Minnesota

for the last 500 years. The stalagmite retains a record of multiple flood layers, rich in magnetic minerals, each of which appears to be associated with an extreme precipitation event. A time series of magnetization peaks acquired with a scanning SQUID microscope, yields an average flood recurrence rate of $\leq$5 events per century for the last 500 years. This rate increases to $\sim$7 events per century since 1900, coincident with historical timber and agricultural land-use changes in Minnesota. The flood layers after 1900 also appear broader than those preceding 1900, suggesting that higher concentrations of fine grained sediment were transported into the cave during normal background dripwater conditions, perhaps linked to land-use changes that broke up and loosened regional soils in a manner that was not observed prior to 1900. Thus, the magnetic record within speleothems at Spring Valley Caverns suggests that modest climate change and human land use variability can increase the rate at which surface sediments are transported into underlying karst systems. Our results offer a rapid, new geophysical technique for compiling detailed paleoflood records from speleothems and may be useful for illustrating how flood recurrence rates have evolved from deep time to the present.

Declaration of competing interest

The authors declare that they have no known competing financial interests or personal relationships that could have appeared to influence the work reported in this paper.

Acknowledgements

This work was financially supported by US National Science Foundation grant EAR-1316385 and through a University of Minnesota Grants-In-Aid award and a McKnight Land-Grant Professorship awarded to JMF. EAL and BPW would like to thank the National Science Foundation grants DMS-1521765 and DMS-0934689 for partial support. We thank John Ackerman, the owner of Spring Valley Caverns, for access to, and his continued support of research in Spring Valley Caverns. We are grateful for comments by Andrew Roberts, Plinio Jaqueto, and an anonymous reviewer. This is IRM contribution 1309.

References

Baker, V.R., 1973. Paleohydrology of the Missoula Floods. In: Paleohydrology and Sedimentology of Lake Missoula Flooding in Eastern Washington. In: Special Paper, vol. 144. Geol. Soc. Am., Boulder, Colorado, pp. 13–32.

Baudenbacher, F., Fong, L.E., Holzer, J.R., Radparvar, M., 2003. Monolithic low-transition- temperature superconducting magnetometers for high resolution imaging magnetic fields of room temperature samples. Appl. Phys. Lett. 82, 3487–3489. https://doi.org/10.1063/1.1572968.

Cheng, H., Edwards, R.L., Shen, C.C., Polyak, V.J., Asmerom, Y., Woodhead, J., Hellstrom, J., Wang, Y., Kong, X., Spötl, C., Wang, X., Alexander, E.C., 2013. Improvements in ^{230}Th dating, ^{230}Th and ^{234}U half-life values, and U-Th isotopic measurements by multi-collector inductively coupled plasma mass spectrometry. Earth Planet. Sci. Lett. 371–372, 82–91. https://doi.org/10.1016/j.epsl.2013.04.006.

Committee on Levees and the National Flood Insurance Program Improving Policies and Practices, Water Science and Technology Board, Division on Earth and Life Studies, National Research, 2013. Levees and the National Flood Insurance Program: Improving Policies and Practices. The National Academies Press. ISBN 9780309282901, 258 p.

Dasgupta, S., Saar, M.O., Edwards, R.L., Shen, C., Cheng, H., Alexander, E.C., 2010. Three thousand years of extreme rainfall events recorded in stalagmites from Spring Valley Caverns, Minnesota. Earth Planet. Sci. Lett. 300 (1–2), 46–54. https://doi.org/10.1016/j.epsl.2010.09.032.

Denniston, R.F., Luetscher, M., 2017. Speleothems as high-resolution paleoflood archives. Quat. Sci. Rev. 170, 1–13. https://doi.org/10.1016/j.quascirev.2017.05.006.

Dorale, J.A., Edwards, R.L., Alexander, E.C., Shen, C., Richards, D.A., Cheng, H., 2004. Uranium-series dating of speleothems: current techniques, limits, & applications. In: Sasowsky, I., Mylroie, J. (Eds.), Studies of Cave Sediments: Physical and Chemical Records of Paleoclimate. Springer, Dordrecht, Netherlands, pp. 177–197.

Edwards, R.L., Gallup, C.D., Cheng, H., 2003. Uranium-series dating of marine and lacustrine carbonates. In: Bourdon, B., Henderson, G.M., Lundstrom, C.C., Turner, S.P. (Eds.), Reviews in Mineralogy and Geochemistry: Uranium-Series Geochemistry. Mineralogical Society of America, Washington, DC, United States of America, pp. 363–405.

Engstrom, D.R., Almendinger, J.E., Wolin, J.A., 2009. Historical changes in sediment and phosphorus loading to the upper Mississippi River: mass-balance reconstructions from the sediments of Lake Pepin. J. Paleolimnol. 41, 563–588.

Finné, M., Kylander, M., Boyd, M., Sundqvist, H.S., Löwemark, L., 2014. Can XRF scanning of speleothems be used as a non-destructive method to identify paleoflood events in caves? Int. J. Speleol. 44 (1), 17–23. https://doi.org/10.5038/1827-806X.44.1.2.

Fong, L.E., Holzer, J.R., McBride, K.K., Lima, E.A., Baudenbacher, F., 2005. High resolution room-temperature sample scanning superconducting quantum interference device microscope configurable for geological and biomagnetic applications. Rev. Sci. Instrum. 76. https://doi.org/10.1063/1.1884025.

Frappier, A.B., Pyburn, J., Pinkey-Drobnis, A.D., Wang, X., Corbett, D.R., Dahlin, B.H., 2014. Two millennia of tropical cyclone-induced mud layers in a northern Yucatán stalagmite: multiple overlapping climatic hazards during the Maya Terminal Classic "megadroughts". Geophys. Res. Lett. 41, 5148–5157. https://doi.org/10.1002/2014GL059882.

Gazquez, F., Calaforra, J.M., Forti, P., Stoll, H., Ghaleb, B., Delgado-Huertas, A., 2014. Paleoflood events recorded in speleothems in caves. Earth Surf. Process. Landf. 39, 1345–1353. https://doi.org/10.1002/esp.3543.

González-Lemos, S., Müller, Wolfgang, Pisonero Hai Cheng, Jorge, Lawrence Edwards, R., Stoll, Heather M., 2015. Holocene flood frequency reconstruction from speleothems in northern Spain. Quat. Sci. Rev. 127, 129–140. https://doi.org/10.1016/j.quascirev.2015.06.002.

Knox, J.C., 1985. Responses of floods to Holocene climatic change in the upper Mississippi Valley. Quat. Res. 23, 287–300. https://doi.org/10.1016/0033-5894(85)90036-5.

Knox, J.C., 1993. Large increases in flood magnitude in response to modest climate change. Nature 361, 430–432.

Knox, J.C., 2000. Sensitivity of modern and Holocene floods to climate change. Quat. Sci. Rev. 19, 439–457. https://doi.org/10.1016/S0277-3791(99)00074-8.

Larson, A.M., 2007. The White Pine Industry in Minnesota: A History. University of Minnesota Press, Minneapolis, 432 pp.

Lascu, I., Feinberg, J.M., 2011. Speleothem magnetism. Quat. Sci. Rev. 30 (23–24), 3306–3320. https://doi.org/10.1016/j.quascirev.2011.08.004.

Lima, E.A., Weiss, B.P., 2016. Ultra-high sensitivity moment magnetometry of geological samples using magnetic microscopy. Geochem. Geophys. Geosyst. 17. https://doi.org/10.1002/2016GC006487.

Lima, E.A., Weiss, B.P., Baratchart, L., Hardin, D.P., Saff, E.B., 2013. Fast inversion of magnetic field maps of unidirectional planar geological magnetization. J. Geophys. Res., Solid Earth 118 (6), 2723–2752. https://doi.org/10.1002/jgrb.50229.

Novotny, E.V., Stefan, H.G., 2007. Stream flow in Minnesota: indicator of climate change. J. Hydrol. 334, 319–333. https://doi.org/10.1016/j.jhydrol.2006.10.011.

Ross, A., 1856. The Red River Settlement: Its Rise, Progress and Present State. Smith Elder and Co., London, 448 p.

St. George, S., Nielsen, E., 2002. Flood ring evidence and its application to paleoflood hydrology of the Red River and Assiniboine River in Manitoba. Géogr. Phys. Quat. 56 (2–3), 181–190. https://doi.org/10.7202/009104ar.

St. George, S., Nielsen, E., 2003. Palaeoflood records for the Red River, Manitoba, Canada, derived from anatomical tree-ring signatures. Holocene 13 (4), 547–555. https://doi.org/10.1191/0959683603hl645rp.

Strauss, B.E., Strehleu, J.H., Lascu, I., Dorale, J.A., Penn, R.L., Feinberg, J.M., 2013. The origin of magnetic remanence in stalagmites: observations from electron microscopy and rock magnetism. Geochem. Geophys. Geosyst. 14 (12), 5006–5025. https://doi.org/10.1002/2013GC004950.

Umbanhowar, C.E., Camill, P., Dorale, J.A., 2011. Regional heterogeneity and the effects of land use and climate on 20 lakes in the big woods region of Minnesota. J. Paleolimnol. 45 (2), 151–166. https://doi.org/10.1007/s10933-010-9486-5.

Weiss, B.P., Lima, E.A., Fong, L.E., Baudenbacher, F.J., 2007. Paleomagnetic analysis using SQUID microscopy. J. Geophys. Res. 112, B09105. https://doi.org/10.1029/2007JB004940.